Effect of High and Low-Pressure Exhaust Gas Recirculation System on NOx Emissions in a Bus Diesel Engine

Dinh Xuan Thanh

Department of Automobile Engineering, Hanoi University of Industry, No 298 Cau Dien Street, Minh Khai Ward, Bac Tu Liem District, Hanoi City, Vietnam

Abstract: ***This study aims to design the exhaust gas recirculation (EGR) system for a bus diesel engine in order to reduce exhaust emissions. This includes the experiment and simulation of the test engine based on the Emission Test Cycles ECE-R49. The comparison of high and low-pressure exhaust gas recirculation systems fitted on a bus engine was conducted to analyze the effects of their control on fuel consumption, pollutant emissions. The research results showed that the test engine retrofitted high-pressure exhaust gas recirculation systems (H-EGR) results in a lower ratio of EGR in comparison with that of low-pressure exhaust gas recirculation systems (L-EGR). In addition, due to the higher intake gas velocity and pressure, the local loss in case of H-EGR is also higher than the one of the L-EGR at the venturi assembly position. The H-EGR was only effective at the engine load less than 75%; consequently, the role in reducing NOx emissions was less effective than that of the L-EGR. The maximum reduction of NOx emissions in case of H-EGR was 41.27% at a load of 75% and a velocity of 1400 rpm. Meanwhile, the NOx emission can be reduced to 62.43% in case of L-EGR.***

Keywords: Exhaust gas recirculation; Fuel consumption enhancement, Diesel engine, Engine characteristic, Nitrogen emissions

1. Introduction

In response to meet global strict requirements for emissions control such as ultra-low emission vehicle and Kyoto Protocol, the automobile manufacturers need to find out the new technology in order to reduce fuel consumption and exhaust emissions from their manufactured vehicles [1]. EGR system has been popularly used as an effective preprocessing means to reduce NOx emissions. The recycled exhaust gas contributes to increasing the mixer's heat capacity, knock control, and supplies pressure to the intake manifold reducing pumping loss. Therefore, when an EGR system is effectively used, positive effects can reduce NOx emission as well as increase fuel consumption efficiency [2-3].

The effect of EGR on diesel engines has been conducted in many previous studies [4–6]. For instance, Giorgio et al studied the synthetic effects of L-EGR and H-EGR on the performance of turbocharged diesel engine [7]. The results showed that the effect of the L-EGR on intake and exhaust parameters is lower than that of the H-EGR loop, resulting in engine and turbocharger working conditions closer to the reference one without EGR. In another research, Ibrahim et al. [8] confirmed that NOx emissions could be reduced up to 50% by adding EGR to the intake charge. In another research, a stronger effect in reducing NOx emission of EGR technology was shown by Schöffler et al. [7], in which a reduction of 80–90% in NOx emissions was obtained when applying EGR system for the test engine. Yang Shuai et al. [8] also performed a simulation of the turbocharged diesel engine retrofitted EGR system, the results showed the EGR system contributed to the reduction of air fuel ratio, cylinder pressure, cylinder temperature and exhaust temperature; as a result, the NOx emissions were dramatically decreased. Starting from the above considerations, this research aims to find out the technology to reduce exhaust emissions of bus vehicles in Vietnam. Consequently, the simulation and experiment test of a bus engine and its EGR systems including H-EGR and L-EGR were conducted at Laboratory of Internal Combustion Engine, Hanoi University of Science and Technology. The test was based on ECE-R49 driving cycle procedure to evaluate fully the effect of EGR system at the full-range operation of the test engine.

2. Test Engine, Test Fuel, and Test Driving Cycle

2.1. Test Engine Fuel Characteristics

The test engine is a four-stroke diesel engine retrofitting for a popular bus model in Vietnam, with the rated output 140 kW/2200 rpm. Table 1 shows the characteristics of the test engine:

Table 1: The parameter characteristics of the test engine

No	Parameter	Value	Unit
1	Firing order	1-3-5-6-2-4	-
3	Diameter	139	mm
4	Stroke piston	111	mm
5	Connecting rod	230	mm
6	Compression Ratio	16.4	-
7	Rated power	140	kW
8	Maximum torque	740	N.m
9	Injection timing	16	Degree

Table 2: The parameter characteristics of the test fuel

No	Fuel Property	Value	Unit
1	Sulphur Content (mg/kg)	0.05%	mg/kg
2	Cetane Index	47	-
3	Flash Point	56	(^{0}C)
4	Viscosity at 40 ^{0}C	2.8	(cSt)
5	Carbon residue	0.28	(10% btms)
6	Ash (% weight)	0.01	(% weight)
7	Water Content	190	(mg/kg)
8	Particulate Contaminant	9.7	(mg/l)
9	Density at 15 ^{0}C	848	(kg/m^3)

2.2. Test driving cycle

The experiment and simulation of the test engine in this research were performed based on the ECE-R40 driving cycle. The ECE-R49 is a 13-mode steady-state diesel engine test cycle introduced by ECE Regulation No. 49 and then adopted by Directive 88/77/EEC with the characteristic shown in Table 3 and Fig. 1 [11]:

Table 3: ECE-R49 driving cycle characteristics

Mode No.	Engine speed	Load, %	Weighting factors
1	Idle	-	0.25/3
2	Maximum torque speed	10	0.08
3		25	0.08
4		50	0.08
5		75	0.08
6		100	0.25
7	Idle	-	0.25/3
8	Rated power speed	100	0.1
9		75	0.02
10		50	0.02
11		25	0.02
12		10	0.02
13	Idle	-	0.25/3

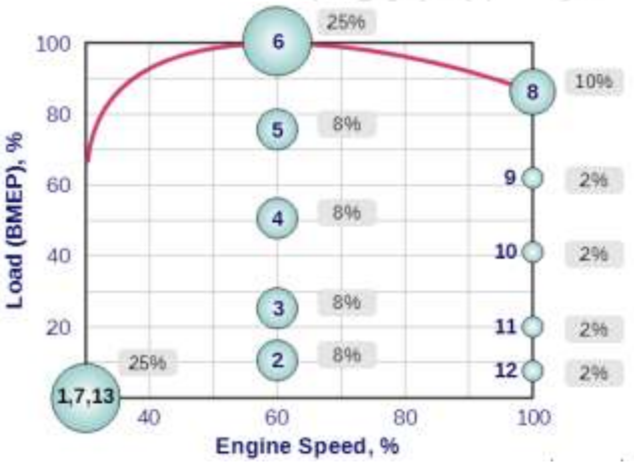

Figure 1: ECE-R49 driving cycle

3. Simulation Test Procedure

3.1. Theoretical basis and governing equation

3.1.1. Basic conservation equations

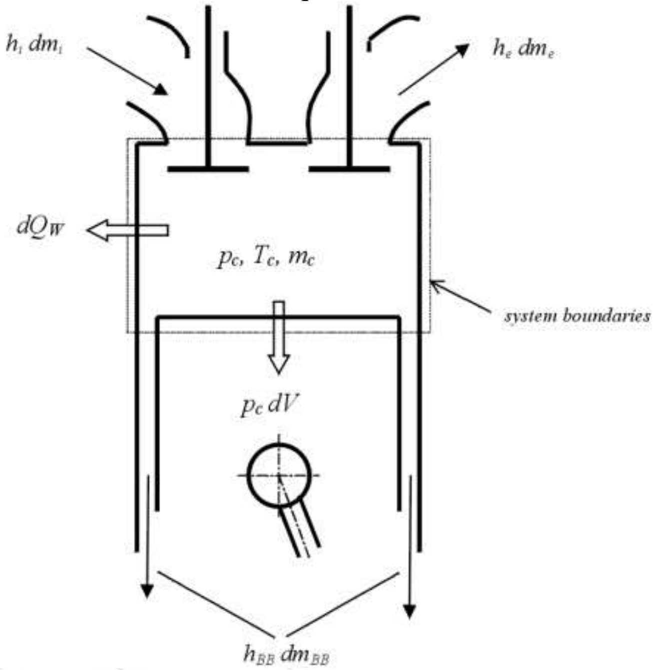

Figure 2: Energy Balance of Cylinder [9-10]

Fig. 2 shows the calculation of energy balance of an internal combustion engine. Where α is the crank angle, hi the enthalpy of the in-flowing mass, dmi is the mass element flowing into the cylinder, he is the enthalpy of the mass leaving the cylinder, dme is the mass element flowing out of the cylinder, h_{BB} is the enthalpy of blow-by, dm_{BB} is the mass element of blow, Q_w is the wall heat loss, p_c, T_c, m_c, V is the cylinder pressure, cylinder temperature, mass in the cylinder pressure and cylinder volume, respectively.

The calculation of the thermodynamic state of the cylinder is based on the first law of thermodynamics as shown in Eq. 1 [9, 10]:

$$\frac{d(m_C.u)}{d\alpha} = -p_C.\frac{dV}{d\alpha} + \frac{dQ_F}{d\alpha} - \sum\frac{dQ_W}{d\alpha} - h_{BB}.\frac{dm_{BB}}{d\alpha} \quad (1)$$

The mass flow rates at the intake and exhaust ports are calculated from the Equations for isentropic orifice flow under consideration of the flow efficiencies of the ports determined on the steady state flow test rig. From the energy Equation for steady state orifice flow, the Equation for the mass flow rates is as follows:

$$\frac{d_m}{d_t} = A.p_0.\sqrt{\frac{2}{R_0 T_0}}.\psi \quad (2)$$

where d_m/d_t is the mass flow rate, A is the effective flow area, p_0 is the upstream stagnation pressure, T_0 is the upstream stagnation temperature, R_0 is the gas constant, and ψ is determined from Equation 3 for subsonic flow:

$$\psi = \sqrt{\frac{k}{k-1}\left[\left(\frac{p_2}{p_1}\right)^{\frac{2}{k}} - \left(\frac{p_2}{p_1}\right)\frac{k+1}{k}\right]} \quad (3)$$

where p_2 and k are the downstream static pressure and ratio of specific heats, respectively.

3.1.2. Combustion Model

BOOST SOFTWARE uses the Mixing Controlled Combustion (MCC) model for the prediction of the combustion characteristics in direct injection compression ignition engines [9,10]. The heat release is a function of the fuel quantity available (f_1) and the turbulent kinetic energy density (f_2), Eq. 2.

$$\frac{dQ}{d\phi} = C_{Comb}\cdot f_1(M_F, Q)\cdot f_2(k,V) \qquad (4)$$

Where $f_1(M_F, Q) = M_F - \frac{Q}{LVC}$, $f_2(k,V) = \exp(C_{rate}\cdot \frac{\sqrt{k}}{\sqrt[3]{V}})$,

C_{Comb} - combustion constant [kJ/kg.deg CA], C_{rate} - mixing rate constant [s], k - local density of turbulent kinetic energy [m^2/s^2], M_F - vaporized fuel mass [kg], LCV - lower heating value [kJ/kg], Q - cumulative heat release for the mixture controlled combustion [kJ], V - cylinder volume [m^3], α - crank angle [deg CA].

3.1.3. Heat Transfer Model

The heat transfer to the walls of the combustion cham-ber, i.e. the cylinder head, the piston, and the cylinder liner, is calculated from Eq. (3) [9-10].

$$Q_{wi} = A_i \cdot \alpha_i \cdot (T_c - T_{wi}) \qquad (5)$$

where Q_{wi} - wall heat flow, A_i - surface area, α_i - heat transfer coefficient, T_c gas temperature in the cylinder, T_{wi} - wall temperature.

3.1.4. Turbocharger simulation

For the simulation of a turbine, the performance characteristics along a line of the constant turbine are required. The power provided by the turbine is determined by the turbine mass flow rate and the enthalpy difference over the turbine.

$$P_T = \overline{\dot{m}.\eta_m.(h_3 - h_4)} \qquad (6)$$

where P_T - turbine power, $\dot{m}$ - turbine mass flow, η_m - mechanical efficiency of the turbocharger, h_3 - enthalpy at the turbine inlet, h_4 - enthalpy at the turbine outlet

$$h_3 - h_4 = \eta_{s,T}.c_p.T_3.\left[1 - \left(\frac{p_4}{p_3}\right)^{\frac{K-1}{K}}\right] \qquad (7)$$

where $\eta_{s,T}$ - isentropic turbine efficiency, Cp - mean specific heat at a constant pressure between turbine inlet and outlet, T_3 - turbine inlet temperature, p_4/p_3 - turbine expansion ratio, η_{tot} - total efficiency of the turbine = $\eta_m.\ \eta_{s,T}$.

The power consumption of the turbo compressor depends on the mass flow rates in the compressor and the enthalpy difference over the compressor. The latter is influenced by the pressure ratio, the inlet air temperature, and the isentropic efficiency of the compressor.

$$P_c = \overline{\dot{m}.(h_2 - h_1)} \qquad (8)$$

where P_c - compressor power consumption, $\dot{m}_c$ - mass flow rate in the compressor, h_2 - enthalpy at the outlet of the compressor, h_1 - enthalpy at the inlet to the compressor

$$h_2 - h_1 = \frac{1}{\eta_{s,c}}.c_p.T_1.\left[\left(\frac{p_2}{p_1}\right)^{\frac{K-1}{K}} - 1\right] \qquad (9)$$

Where $\eta_{s,c}$ - isentropic efficiency of the compressor, c_p - mean value of the specific heat at a constant pressure between compressor inlet and outlet, T_1 - compressor inlet temperature; p_2/p_1 - compressor pressure ratio.

For steady state engine operation, the performance of the turbocharger is determined by the energy balance or the first law of thermodynamics. The mean power consumption of the compressor must be equal to the mean power provided by the turbine.

3.2. Test engine model in AVL Boost software

The model is built based on the structure of the existing test engine and the relative document. Table 4 shows some elements and parameters of the model.

Table 4: Some elements of the test engine model

No	Element Name	Symbol
1	Intake, Exhaust pipe	-
2	Boundary elements	SB
3	Plenum	PL
4	Cylinder	C
5	Restriction	R
6	Measuring point	MP
7	Air cleaner	CL
8	Turbocharger	TC
9	Wastegate	WG
10	Air cooler	CL
11	Air cleaner	CO

Fig. 3 and Fig. 4 show the test engine modeled in AVL-Boost software corresponding to L-EGR and H-EGR system

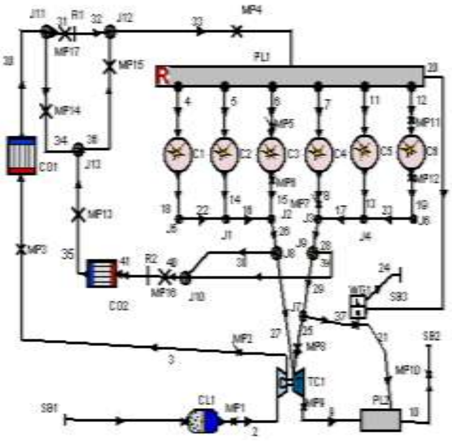

Figure 3: The engine test model retrofitted H-EGR system

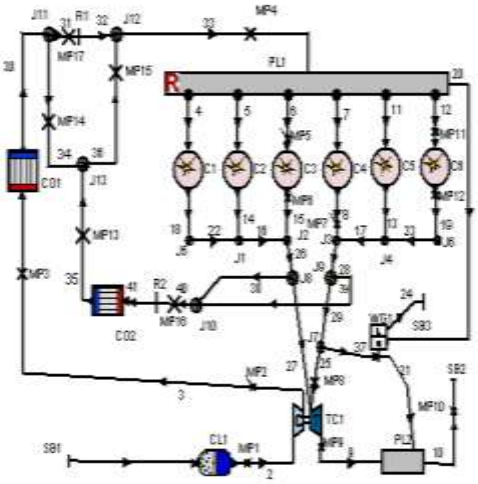

Figure 4: The engine test model retrofitted L-EGR system

4. Experimental Setup of the Test Engine

The experimental setup to evaluate the performance of the test engine. Fig. 5 shows the experimental setup conducted in Lab of Internal Combustion Engine, Hanoi University of Science and Technology, Vietnam. Testing equipment includes a test engine, chassis dynamometer, control unit, fuel consumption device, air flow measurement instrument, and temperature sensors. To conduct the specific engine speed, the experiments were conducted with the single cylinder diesel engine corresponding to various engine speeds.

Figure 5: Experimental setup of the test engine

5. Results and Discussion

5.1. Validation of the simulation model

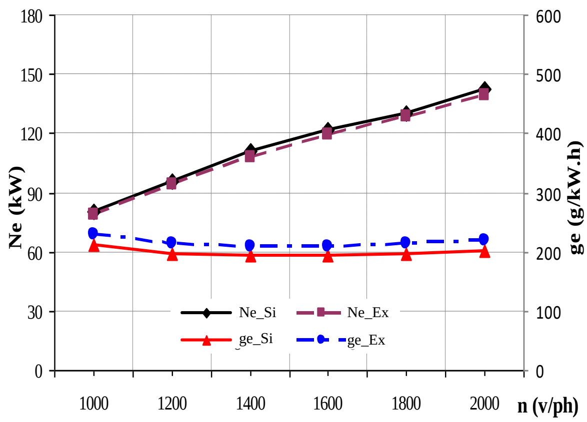

Figure 6: Validation of the simulation model

Fig. 6 shows the results of simulation and experiment test. There is a good agreement between simulation and experiment results, the maximum difference of the fuel consumption is less than 5.2% and about 3% of the power. The difference isn't too much, the results are enough reliability to serve for the continuous researching. Slight differences between the simulation and experimental data are caused by the assumptions used in the simulation. However, the differences are very small; then the simulation models of test engine can be used to model the test engine retrofitted EGR system.

5.2. Effect of H-EGR and L-EGR system on NOx emissions

5.2.1. Effect of H-EGR and L-EGR on the EGR ratio

Table 5: The EGR ratio of the test engine retrofitted H-EGR and L-EGR system according to ECE-R49 driving cycle

Mode No.	Engine speed	Load (%)	Time (min)	% EGR of H-EGR	% EGR of L-EGR	EGR valve open (%)
1	Idle	-	6	0	0	0
2	Rated torque speed	10	6	0	19.38	100
3		25	6	17.52	19.29	100
4		50	6	13.04	18.64	100
5		75	6	10.23	18.39	100
6		100	6	0	18.40	96
7	Idle	-	6	0	0	0
8	Rated power speed	100	6	0	18.15	94
9		75	6	8.15	17.99	100
10		50	6	11.92	18.28	100
11		25	6	17.08	18.31	100
12		10	6	0	18.22	100
13	Idle	-	6	0	0	0

At 10% of the engine load, the exhaust gas pressure at the EGR is lower the pressure at the venturi assembly position, then the exhaust cannot reach to the intake port in case of the H-EGR. Consequently, it is not effective for the NOx reduction. When increasing the engine load, the velocity of the intake gas into the cylinders also increase; as a result, the EGR ratio is reduced. Meanwhile, when the load reaches 100%, the EGR pressure will be lower than the intake gas pressure, then EGR gas cannot reach to the intake port.

The simulation results also showed that the EGR ratio of H-EGR is dramatically lower than that of L-EGR in case of retrofitting for the turbocharged engines.

5.2.2. Effect of H-EGR and L-EGR on NOx emissions

Fig. 7 shows the NOx emissions of the original engine, and the engine retrofitted H-EGR and L-EGR system.

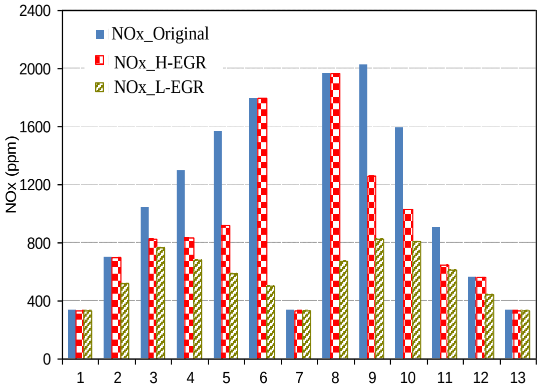

Figure 7: Effect of H-EGR and L-EGR on NOx emissions

In case of the H-EGR, it is only effective at a load of 25%, 50%, and 70%, furthermore and the EGR ratio is lower than that of L-EGR; then its NOx emissions reduction is lower than L-EGR. The maximum of the NOx emissions reduction was approximately 41% at the load of 75% and 1400 rpm. However, with the same engine operation point, the NOx emissions reduction was 62% in case of L-EGR. On the other hand, at 10% and 100% of the load, the EGR gas cannot reach to the intake port, then the NOx emissions were still high.

Table 6: Simulation results of NOx emissions of the test engine according to ECR-R49 driving cycle

Unit	Original	H-EGR	L-EGR	Euro II standard
g/kW.h	14.532	13.55	6.015	7.0

As illustrated in Table 5, in case of H-EGR, the NOx emission was reduced about 6.77% in average compared to the original test engine and it also did not satisfy Euro standard applying for heavy truck vehicles. Meanwhile, NOx emission was reduced up to 58.61% when applying L-EGR for the test engine and it responded Euro II standard. Consequently, retrofitting L-EGR system for the test engine can solve the NOx emissions problem to respond Euro II standard.

6. Conclusions

The objective of this study is to reduce NOx emissions with EGR system in diesel engine at the modified transient mode. The preliminary studies were conducted to investigate the basic characteristics of engine components such as the cooled EGR system. The application of EGR system can dramatically reduce NOx emission. The L-EGR is more effective than that of H-EGR when applying them to turbocharged engines. However, when applying this method, it will produce higher particulate matter (PM) emissions. Consequently, it is recommended that the treatment to reduce PM emission should be applied to solve the above problem.

References

[1] Koike. M.; Saito. A. Research and development of a new direct injection gasoline engine. SAE 2000. 2000-01-0530.
[2] Benson R.S. The thermodynamics and gas dynamics of internal-combustion engines. 3rd ed.; Clarendon Press: Oxford. The United Kingdom. 1986.
[3] Park. S.-H.; Lee. J.; Kim. K.; Park S.; Kim. H.-M. Experimental characterization of cooled EGR in a gasoline direct injection engine for reducing fuel consumption and nitrogen oxide emission. Heat Mass Transfer 2015. 51. 1639–1651.
[4] U. Lundqvist. G. Smedler. P. Stalhammar. A comparison between different EGR systems for HD Diesel engines and their effect on performance, fuel consumption and emissions. In: Proceedings of the SAE world congress. Detroit. MI. USA. SAE paper 2000–01-0226; 2000.
[5] S. Langridge. H. Fessler. Strategies for high EGR rates in a diesel engine. In: Proceedings of the SAE world congress & exhibition. Detroit. MI. USA. SAE paper 2002–01-0961 (2002).
[6] O. Vítek. J. Macek. M. Polá?ek. S. Schmerbeck T. Kammerdiener. Comparison of different EGR solutions. In: Proceedings of the SAE world congress & exhibition. Detroit. MI. USA. SAE paper 2008-01-0206; 2008.
[7] Giorgio Zamboni. Massimo Capobianco. Experimental study on the effects of HP and LP EGR in an automotive turbocharged diesel engine. Appl. Energy. 94 (2012). pp. 117-128.
[8] A. Ibrahim. S. Bari. An experimental investigation on the use of EGR in a supercharged natural gas SI engine. Fuel. 89 (2010). pp. 1721–1730
[9] AVL: Thermodynamic cycle simulation Boost. Primary. Version 3.2 1998
[10] AVL: Thermodynamic cycle simulation Boost. Boost user's guide. Version 3.2
[11] https://www.dieselnet.com/standards/cycles/ece_r49.php

Author Profile

Dr. Dinh Xuan Thanh received the B.S. and M.S. degrees in Mechanical Engineering from Hanoi University of Science and Technology in 2000 and 2004, respectively. During 2007-2011, he studied and worked in Laboratory of Internal Combustion Engine, Hanoi University of Science and Technology for his Ph.D. degree. Now, he is a Professor in Hanoi University of Industry. His research interests focus on the internal combustion engine design, Exhaust emissions reduction, and Renewable energy.